

Mass spectrum and decay constants of radially excited vector mesons

Fredy F. Mojica,^{1,*} Carlos E. Vera,^{1,†} Eduardo Rojas,^{2,‡} and Bruno El-Bennich^{3,§}

¹*Departamento de Física, Facultad de Ciencias, Universidad del Tolima, 730006299, Ibagué, Colombia*

²*Instituto de Física, Universidad de Antioquia, Calle 70 No. 52-21, Medellín, Colombia*

³*Laboratório de Física Teórica e Computacional, Universidade Cruzeiro do Sul, Rua Galvão Bueno, 868, 01506-000 São Paulo, SP, Brazil*

We calculate the masses and weak decay constants of flavorless ground and radially excited $J^P = 1^-$ mesons and the corresponding quantities for the K^* , within a Poincaré covariant continuum framework based on the Bethe-Salpeter equation. We use in both, the quark's gap equation and the meson bound-state equation, an infrared massive and finite interaction in the leading symmetry-preserving truncation. While our numerical results are in rather good agreement with experimental values where they are available, no single parametrization of the QCD inspired interaction reproduces simultaneously the ground and excited mass spectrum, which confirms earlier work on pseudoscalar mesons. This feature being a consequence of the lowest truncation, we pin down the range and strength of the interaction in both cases to identify common qualitative features that may help to tune future interaction models beyond the rainbow-ladder approximation.

PACS numbers: 12.38.-t 11.10.St 11.15.Tk, 14.40.Pq 13.20.Gd 14.40.Df

I. INTRODUCTION

Vector mesons play an important role in the physics of strong interactions and hadron phenomenology. Since these mesons and the photon share the same quantum numbers, $J^{PC} = 1^{--}$, flavorless neutral vector mesons can directly couple to the photon via an electromagnetic current. Historically, this led to the *vector meson dominance model*. Compared to other mesons their production can be measured with very high precision, for instance in electron-positron collisions via the process $e^+e^- \rightarrow \gamma^* \rightarrow \bar{q}q$ which provides a much cleaner signal than hadronic reactions. Notwithstanding complications with hadronic final states, vector mesons are abundant decay products in electroproduction of excited nucleons [1, 2], N^* , and exclusive vector meson production reactions are responsible for a large fraction of the total hadronic cross section and precede di-lepton decays in relativistic heavy-ion collisions [3]. In flavor physics, exclusive B decays with final-state vector mesons, e.g. $B \rightarrow V\pi$, $B \rightarrow V\ell\nu_\ell$, $B \rightarrow V\mu^+\mu^-$ or $B \rightarrow V\gamma$, are a central component of the LHCb experimental program and the $B \rightarrow K^*\mu^+\mu^-$ and $B_s \rightarrow K^*\mu^+\mu^-$ decays are of particular interest, as their angular distributions are very sensitive probes of new physics [4–9]. In the latter cases, a precise knowledge of the pseudoscalar and vector meson light-cone distribution amplitudes is essential [10].

A characteristic feature of the 1^{--} ground-state vector mesons is their predominant occurrence as pure $\bar{q}q$ states: in the case of the $\omega(782)$ and $\phi(1020)$ mesons the vector flavor-nonnet mixing angle is close to ideal mixing, i.e.

$\phi(1020)$ is nearly a pure $|\bar{s}s\rangle$ state and $\omega = (\bar{u}u + \bar{d}d)/\sqrt{2}$. This ideal mixing is not evident in pseudoscalar and scalar meson multiplets. Thus, vector mesons as decay products of heavier non-vector mesons are a very good probe of their flavor content measured in their respective decay rates into different types of mesons.

The study of vector mesons is complementary to that of light pseudoscalar mesons, the Goldstone bosons, as their masses are more in agreement with the sum of their typical constituent quark masses. This stands in contrast to the light pseudoscalar's properties best described by the dichotomy of dynamical chiral symmetry breaking (DCSB), which generates a light-quark mass consistent with typical empirical constituent masses [11–15] even in the chiral limit, yet also produces a very light Goldstone boson due to explicit breaking of chiral symmetry of non-zero current-quark masses. These characteristic features of the light pseudoscalar octet are dictated by an axialvector Ward-Green-Takahashi identity which relates dynamical quantities in the chiral limit. Most chiefly, it implies that the leading Lorentz covariant in the pseudoscalar quark-antiquark γ_5 channel is equal to $B(p^2)/f_\pi$, where $B(p^2)$ is the scalar component of the chiral quark self energy. As a corollary, the two-body problem is solved almost completely once a nontrivial solution of the gap equation is found.

This remarkable fact facilitates the phenomenology of light pseudoscalar and is taken advantage of within the joint approach of the Dyson-Schwinger equation (DSE) and Bethe-Salpeter equation (BSE) in continuum Quantum Chromodynamics (QCD) [2, 16–22]. That is because in both, the two-point and four-point Green functions, the axialvector Ward-Green-Takahashi identity is preserved by their simplest approximation, namely the rainbow-ladder (RL) truncation. There is no reason to expect *a priori* this truncation to be as successful in describing vector mesons whose solutions contain double the amount of covariants and whose higher masses sam-

*Electronic address: fremo22@gmail.com

†Electronic address: cvera@ut.edu.co

‡Electronic address: rojas@gfif.udea.edu.co

§Electronic address: bruno.bennich@cruzeirodosul.edu.br

ple the quark propagator in larger domain of the complex p^2 plane. Moreover, the axialvector Ward-Green-Takahashi identity does not constrain the transverse components of the vector meson Bethe-Salpeter amplitude (BSA). Nonetheless, the simplest truncation carried out with the Maris-Tandy model [23, 24] for the quark-gluon interaction function works remarkably well for the lowest ground-state vector mesons, such as the ρ , ω , K^* and ϕ mesons.

We here reassess the seminal work on vector mesons by Maris and Tandy [24] within a modern understanding of the QCD interactions [25, 26]. This ansatz produces an infrared behavior of the interaction, commonly described by a “dressing function” $\mathcal{G}(k^2)$, that mirrors the decoupling solution found in DSE and lattice studies of the gluon propagator [27–38]. This solution is a bounded and regular function of spacelike momenta with a maximum value at $k^2 = 0$. Our aim is to compute the mass spectrum of the ground and radially excited states of the light, strange and charm vector mesons as well as of vector charmonia and bottomia [39–49] which were also the object of lattice-regularized QCD studies [50–52]; in addition we compute their weak decay constants whose precise knowledge is important in hadronic observables measured by LHCb and FAIR-GSI, for example.

II. BOUND STATES IN THE VECTOR CHANNEL

In analogy with previous work on pseudoscalar ground and excited states [53], we employ the RL truncation in both, the quark’s DSE and the vector meson’s BSE, which is the leading term in a symmetry-preserving truncation scheme. The following two sections detail their respective kernels and lay out the setup for the numerical implementation to compute vector meson properties.

A. Quark Gap Equation

The quark’s gap equation is generally described by the DSE,¹

$$S^{-1}(p) = Z_2(i\gamma \cdot p + m^{\text{bm}}) + Z_1 g^2 \int_k^\Lambda D^{\mu\nu}(q) \frac{\lambda^a}{2} \gamma_\mu S(k) \Gamma_\nu^a(k, p), \quad (1)$$

where $q = k - p$, $Z_{1,2}(\mu, \Lambda)$ are the vertex and quark wavefunction renormalization constants, respectively, and

¹ We employ throughout a Euclidean metric in our notation: $\{\gamma_\mu, \gamma_\nu\} = 2\delta_{\mu\nu}$; $\gamma_\mu^\dagger = \gamma_\mu$; $\gamma_5 = \gamma_4\gamma_1\gamma_2\gamma_3$, $\text{tr}[\gamma_4\gamma_\mu\gamma_\nu\gamma_\rho\gamma_\sigma] = -4\epsilon_{\mu\nu\rho\sigma}$; $\sigma_{\mu\nu} = (i/2)[\gamma_\mu, \gamma_\nu]$; $a \cdot b = \sum_{i=1}^4 a_i b_i$; and P_μ timelike $\Rightarrow P^2 < 0$.

$\int_k^\Lambda \equiv \int^\Lambda d^4k/(2\pi)^4$ represents throughout a Poincaré-invariant regularization of the integral with the regularization mass scale, Λ . Radiative gluon corrections in the second term of Eq. (1) add to the current-quark bare mass, $m^{\text{bm}}(\Lambda)$, where the integral is over the dressed gluon propagator, $D_{\mu\nu}(q)$, and the dressed quark-gluon vertex, $\Gamma_\nu^a(k, p)$; the SU(3) matrices, λ^a , are in the fundamental representation. The gluon propagator is purely transversal in Landau gauge,

$$D_{\mu\nu}^{ab}(q) = \delta^{ab} \left(g_{\mu\nu} - \frac{k_\mu k_\nu}{q^2} \right) \frac{\Delta(q^2)}{q^2}, \quad (2)$$

where $\Delta(k^2)$ is the gluon-dressing function. In RL approximation, the quark-gluon vertex is simply given by its perturbative limit,

$$\Gamma_\mu^a(k, p) = \frac{\lambda^a}{2} Z_1 \gamma_\mu, \quad (3)$$

and since we neglect the three-gluon vertex and work in the “Abelian” version of QCD which enforces a Ward-Green-Takahashi identity [23, 54, 55], $Z_1 = Z_2$, we re-express the kernel of Eq. (1),

$$Z_1 g^2 D_{\mu\nu}(q) \Gamma_\mu(k, p) = Z_2^2 \mathcal{G}(q^2) D_{\mu\nu}^{\text{free}}(q) \gamma_\mu, \quad (4)$$

where we suppress color factors and $D_{\mu\nu}^{\text{free}}(q) := (g_{\mu\nu} - q_\mu q_\nu / q^2) / q^2$ is the free gluon propagator. An effective model coupling, whose momentum-dependence is congruent with DSE- and lattice-QCD results and yields successful explanations of numerous hadron observables [2, 22, 53, 56], is given by the sum of two scale-distinct contributions:

$$\frac{\mathcal{G}(q^2)}{q^2} = \frac{8\pi^2}{\omega^4} D e^{-q^2/\omega^2} + \frac{8\pi^2 \gamma_m \mathcal{F}(q^2)}{\ln \left[\tau + (1 + q^2/\Lambda_{\text{QCD}}^2)^2 \right]}, \quad (5)$$

The first term is an infrared-massive and finite *ansatz* for the interaction, where $\gamma_m = 12/(33 - 2N_f)$, $N_f = 4$, $\Lambda_{\text{QCD}} = 0.234$ GeV; $\tau = e^2 - 1$; and $\mathcal{F}(q^2) = [1 - \exp(-q^2/4m_t^2)]/q^2$, $m_t = 0.5$ GeV. The parameters ω and D control the width and strength of the interaction, respectively. At first sight they seem to be independent, yet a large collection of observables of ground-state vector and isospin-nonzero pseudoscalar mesons are practically insensitive to variations of $\omega \in [0.4, 0.6]$ GeV, as long as $D\omega = \text{constant}$. The second term in Eq. (5) is a bounded, monotonically decreasing continuation of the perturbative-QCD running coupling for all spacelike values of q^2 . The most important feature of this *ansatz* is that it provides sufficient strength to realize DCSB and implements a confined-gluon interaction [22]. At $k^2 \gtrsim 2$ GeV², the perturbative component dominates the interaction. In Figure 1 we plot the interaction, $\mathcal{G}(q^2)$ in Eq. (5) for a typical value, $wD = (0.8 \text{ GeV})^3$ and $\omega = 0.4$ [53], employed in RL approximation as well as for other values of ω to illustrate the decrease of and shift towards larger k^2 of its strength. For $\omega \simeq 0.6$, the

B. Vector Bound-State Equation

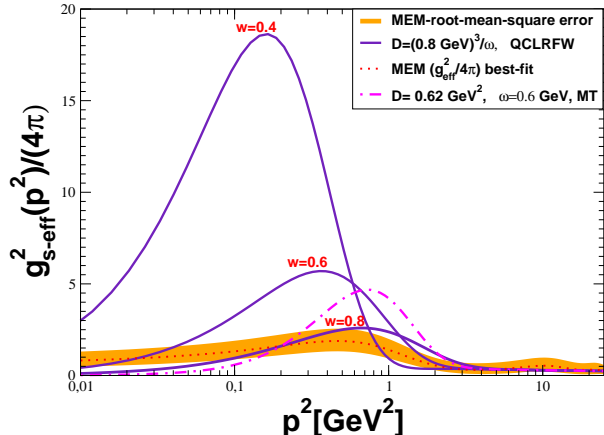


FIG. 1: (Color online) The solid indigo curves correspond to the effective coupling strength \mathcal{G} in Ref. [25] with $wD = (0.8 \text{ GeV})^3$; the dashed-dotted magenta curve depicts the effective strength in the Maris-Tandy model [24]; the dotted red curve corresponds to the effective strength extracted from lattice QCD data by using the maximum entropy method (MEM); see Ref. [57] for details.

functional form of the interaction is more akin to that employed in combination with a ghost-dressed Ball-Chiu vertex [57–59].

The solutions for spacelike momenta, $p^2 > 0$, of the gap equation (1) include a vector and a scalar piece,

$$S_f^{-1}(p) = i \gamma \cdot p A_f(p^2) + \mathbf{1}_D B_f(p^2), \quad (6)$$

for a given flavor, f , which requires a renormalization condition for the quark's wave function,

$$Z_f(p^2) = 1/A_f(p^2)|_{p^2=4 \text{ GeV}^2} = 1. \quad (7)$$

This imposed condition is supported by lattice-QCD simulations of the dressed-quark propagator. The mass function, $M_f(p^2) = B_f(p^2, \mu^2)/A_f(p^2, \mu^2)$, is renormalization-point independent. In order to reproduce the quark-mass value in perturbative QCD, another renormalization condition is imposed,

$$S_f^{-1}(p)|_{p^2=\mu^2} = i \gamma \cdot p + \mathbf{1}_D m_f(\mu), \quad (8)$$

at a large spacelike renormalization point, $\mu^2 \gg \Lambda_{\text{QCD}}^2$, where $m_f(\mu)$ is the renormalized running quark mass:

$$Z_m^f(\mu, \Lambda) m_f(\mu) = m_f^{\text{bm}}(\Lambda). \quad (9)$$

Here, $Z_m^f(\mu, \Lambda) = Z_4^f(\mu, \Lambda)/Z_2^f(\mu, \Lambda)$ is the flavor dependent mass-renormalization constant and $Z_4^f(\mu, \Lambda)$ is associated with the mass term in Lagrangian. In particular, $m_f(\mu)$ is nothing else but the dressed-quark mass function evaluated at one particular deep spacelike point, $p^2 = \mu^2$, namely: $m_f(\mu) = M_f(\mu)$.

The wave function of a bound state of a quark of flavor, f , and an antiquark of flavor, \bar{g} , in the 1^- channel is related to their BSA, $\Gamma_{V\mu}^{f\bar{g}}(p, P)$, which for a relative momentum, p , and total momentum, P , is obtained from the homogeneous BSE,

$$\Gamma_{\mu}^V(p, P) = \int_k^{\Lambda} \mathcal{K}(p, k, P) S_f(k_+) \Gamma_{\mu}^V(k, P) S_{\bar{g}}(k_-), \quad (10)$$

where $k_+ = k + \eta_+ P$, $k_- = k - \eta_- P$; $\eta_+ + \eta_- = 1$. We employ a ladder truncation of the BSE kernel consistent with that of the quark's DSE (4),

$$\mathcal{K}(p, k, P) = -Z_2^2 \mathcal{G}(q^2) \frac{\lambda^a}{2} \gamma_{\mu} D_{\mu\nu}^{\text{free}}(q) \frac{\lambda^a}{2} \gamma_{\nu}, \quad (11)$$

which satisfies an axial-vector Ward-Green-Takahashi identity [60] and consequently the pseudoscalar mesons are massless in the chiral limit. The BSE defines an eigenvalue problem with physical on-shell solutions for $P^2 = -M_{V_0}^2$ for the ground state and for the radially excited states, $P^2 = -M_{V_n}^2$, $M_{V_{n+1}}^2 > M_{V_n}^2$, $n = 1, 2, 3, \dots$

As we are interested in radially excited $J^P = 1^-$ states, the question arises whether they can be described by the interaction in Eq. (5) with exactly the same parameter set as for ground states, whether the parameters have to be adjusted or whether the truncation fails to achieve at least a reasonable description of their mass spectrum. The masses and weak decay constants of excited states are very sensitive to the strength and width of the long-range term in Eq. (5), which provides more support at large inter-quark separation than, e.g., the Maris-Tandy model [24]. In here, we extend the studies of Refs. [25, 53] to the excited states of vector mesons with an interaction that differs from those employed in Ref. [48]. We also refer to the discussion in Ref. [61], where it is pointed out that beyond-RL contributions are important in heavy-light mesons due to the strikingly different impact of the quark-gluon vertex dressing for a light and a heavy quark. The effects of DSCB and the importance of other quark-gluon tensor structures are increasingly more important for lighter quarks [22, 55]. Thus, one does not expect the RL truncation to accurately describe either the ground nor the excited states of charm and beauty mesons. On the other hand, the RL approximation describes very well equal-mass bound states, such as quarkonia [40–48].

The normalization condition for the Bethe-Salpeter amplitude is,

$$2P_{\mu} = \frac{\partial}{\partial P_{\mu}} \frac{N_c}{3} \int_k^{\Lambda} \text{Tr}_D \left[\bar{\Gamma}_{\nu}^V(k, -K) S_f(k_+) \times \Gamma_{\nu}^V(k, K) S_{\bar{g}}(k_-) \right]_{K=P}^{P^2 = -M_V^2}, \quad (12)$$

The charge-conjugated BSA is defined as $\bar{\Gamma}(k, -P) := C \Gamma^T(-k, -P) C^T$, where C is the charge conjugation operator.

Finally, the weak decay constant for 1^- meson is defined as,

$$f_V M_V \epsilon_\mu^\lambda(P) = \langle 0 | \bar{q} \gamma_\mu q^f | V(P, \lambda) \rangle, \quad (13)$$

where $\epsilon_\mu^\lambda(P)$ is the meson's polarization vector satisfying $\epsilon_\mu^\lambda \cdot P = 0$ and normalized such that $\epsilon_\mu^{\lambda*} \cdot \epsilon_\mu^\lambda = 3$; Eq. (13) can be expressed as,

$$f_V M_V = \frac{Z_2 N_c}{3} \int_k^\Lambda \text{Tr}_D [\gamma_\mu S_f(k_+) \Gamma_{V\mu}^{f\bar{g}}(k, K) S_{\bar{g}}(k_-)]. \quad (14)$$

III. NUMERICAL IMPLEMENTATION

A. Quark Propagators on the Complex Plane

In solving the BSE (10), the quark propagators with momentum $(k \pm P)^2 = k^2 + 2i\eta_\pm |k| M_V - \eta_\pm^2 M_V^2$, where k is collinear with $P = (\vec{0}, iM_V)$ in the meson's rest frame, must necessarily be treated in the complex plane [48, 53]. Complex-conjugate pole positions of the propagators depend on the analytical form of the interaction and can be represented by analytical expressions based on a complex-conjugate pole model [62]:

$$S(p) = \sum_i^n \left[\frac{z_i}{i\gamma \cdot p + m_i} + \frac{z_i^*}{i\gamma \cdot p + m_i^*} \right]; \quad m_i, z_i \in \mathbb{C}. \quad (15)$$

The propagator in Eq. (15) is pole-less on the real time-like axis and therefore has no Källén-Lehmann representation, which is a sufficient condition to implement confinement [2, 16]. The numerical DSE solutions we obtain on the complex plane [53, 61] can be fitted with $n = 3$ complex-conjugate poles. We solve the BSE (10) both ways, employing full numerical DSE solutions for the quark in the complex plane and the pole model in Eq. (15) and find agreement at the one-percent level for the vector meson masses and decay constants.

With respect to the current-quark masses given by,

$$Z_4^f(\mu, \Lambda) m_f(\mu) = Z_2^f(\mu, \Lambda) m_f^{\text{mb}}(\Lambda), \quad (16)$$

where $Z_4^f(\mu, \Lambda)$ is associated with the mass term in the QCD Lagrangian, $m_u = m_d(\mu), m_s(\mu)$ and $m_c(\mu)$ are fixed in Eq. (1) by requiring that the pion and kaon BSEs produce $m_\pi = 0.138$ GeV and $m_K = 0.493$ GeV, respectively. This, in turn, yields $m_{u,d}(\mu) = 3.4$ MeV, $m_s(\mu) = 82$ MeV, $m_c(\mu) = 0.828$ GeV and $m_b(\mu) = 3.86$ GeV for $\mu = 19$ GeV.

B. Solving the Bethe-Salpeter Equation

The general Poincaré-invariant form of the solutions of Eq. (10) in the vector meson channel and for the eigenvalue trajectory, $P^2 = -M_{V_n}^2$, in a orthogonal base with

respect to the Dirac trace is given by:

$$\Gamma_\mu^{V_n}(q; P) = \sum_{\alpha=1}^8 T_\mu^\alpha(q, P) \mathcal{F}_\alpha^n(q^2, q \cdot P; P^2), \quad (17)$$

with the dimensionless orthogonal Dirac basis [24],

$$T_\mu^1(q, P) = \gamma_\mu^T, \quad (18)$$

$$T_\mu^2(q, P) = \frac{6}{q^2 \sqrt{5}} \left[q_\mu^T (\gamma^T \cdot q) - \frac{1}{3} \gamma_\mu^T (q^T)^2 \right], \quad (19)$$

$$T_\mu^3(q, P) = \frac{2}{qP} \left[q_\mu^T (\gamma \cdot P) \right], \quad (20)$$

$$T_\mu^4(q, P) = \frac{i\sqrt{2}}{qP} \left[\gamma_\mu^T (\gamma \cdot P) (\gamma^T \cdot q) + q_\mu^T (\gamma \cdot P) \right], \quad (21)$$

$$T_\mu^5(q, P) = \frac{2}{q} q_\mu^T, \quad (22)$$

$$T_\mu^6(q, P) = \frac{i}{q\sqrt{2}} \left[\gamma_\mu^T (\gamma^T \cdot q) - (\gamma^T \cdot q) \gamma_\mu^T \right], \quad (23)$$

$$T_\mu^7(q, P) = \frac{i\sqrt{3}}{P\sqrt{5}} (1 - \cos^2 \theta) \left[\gamma_\mu^T (\gamma \cdot P) \right. \quad (24)$$

$$\left. - (\gamma \cdot P) \gamma_\mu^T \right] - \frac{1}{\sqrt{2}} T_\mu^8(q, P), \quad (25)$$

$$T_\mu^8(q, P) = \frac{i2\sqrt{6}}{q^2 P \sqrt{5}} q_\mu^T \gamma^T \cdot q \gamma \cdot P. \quad (26)$$

The C -parity properties of this basis are elucidated elsewhere [24] and the transverse projection, V^T , is defined by,

$$V_\mu^T = V_\mu - \frac{P_\mu (P \cdot V)}{P^2}, \quad (27)$$

with $q \cdot P = qP \cos \theta$. These covariants satisfy the orthonormality condition,

$$\frac{1}{12} \text{Tr}_D [T_\mu^\alpha(q, P) T_\mu^\beta(q, P)] = f_\alpha(\cos \theta) \delta^{\alpha\beta}, \quad (28)$$

where the functions $f_\alpha(z)$ are given by $f_1(z) = 1$, $f_\alpha(z) = \frac{4}{3}(1 - z^2)$ with $\alpha = 3, 4, 5, 6$ and $f_\alpha(z) = \frac{8}{5}(1 - z^2)^2$ for $\alpha = 2, 7, 8$. The normalization constants f_α satisfy:

$$\int_0^\pi d\theta \sin^2 \theta f_\alpha(\cos \theta) = \frac{\pi}{2}. \quad (29)$$

Making use of the covariant decomposition in Eq. (17) and the orthogonality relations (28), the homogeneous BSE (10) with the kernel (11) can be recast in a set of eight coupled-integral equations,

$$\begin{aligned} & \mathcal{F}_\alpha^n(p^2, p \cdot P, P^2) f_\alpha(z) = \\ & - \frac{4}{3} \int_k^\Lambda \mathcal{G}(q^2) D_{\mu\nu}^{\text{free}}(q) \mathcal{F}_\beta^n(k^2, k \cdot P; P^2) \\ & \times \frac{1}{12} \text{Tr}_D [T_\rho^\alpha(p; P) \gamma_\mu S_f(k_+) T_\rho^\beta(k; P) S_{\bar{g}}(k_-) \gamma_\nu]. \quad (30) \end{aligned}$$

This equation can be posed as an eigenvalue problem for a set of eigenvectors $\mathcal{F}^n := \{\mathcal{F}_\alpha^n; \alpha = 1, \dots, 8\}$:

$$\lambda_n(P^2) \mathcal{F}^n = \mathcal{K}(p, k, P) \mathcal{F}^n. \quad (31)$$

For every solution eigenvector, \mathcal{F}^n , there exists a mass, M_{V_n} , such that $\lambda_n(-M_{V_n}^2) = 1$ [53, 56, 63–66]. The set of masses, M_{V_n} , represents the radially excited meson spectrum of quark-antiquark bound states with $J^P = 1^-$. In order to improve a faster convergence in solving the coupled equations (30), we expand the eigenfunction into Chebyshev polynomials,

$$\mathcal{F}_\alpha^n(k^2, k \cdot P; P^2) = \sum_{m=0}^{\infty} \mathcal{F}_{\alpha m}^n(k^2; P^2) U_m(z_k), \quad (32)$$

where the $U_m(z)$ are Chebyshev polynomials of second kind and the angles, $z_k = P \cdot k / (\sqrt{P^2} \sqrt{k^2})$ and $z_p = P \cdot p / (\sqrt{P^2} \sqrt{p^2})$, and momenta, k and p , are discretized [53]. We employ three Chebyshev polynomials for the ground and five for excited states. We solve the eigenvalue problem posed in Eq. (31) by means of the implicitly restarted Arnoldi method, as implemented in the ARPACK library [67] which computes the eigenvalue spectrum for a given $N \times N$ matrix. A practical implementation requires a mapping of the BSE kernel $\mathcal{K}_{\alpha\beta}(p, k, P)$ onto such a square matrix and is described in detail in Ref. [53].

We obtain the eigenvalue spectrum, $\lambda_n(P^2)$, of the kernel in Eq. (30) and the associated eigenvectors, \mathcal{F}^n of the vector meson's BSAs where the root, M_{V_n} , of the equation $\lambda_n(P^2 = -M_{V_n}^2) - 1 = 0$ is found by employing the *Numerical Recipe* [68] subroutines `zbrent` and `rtsec`. We verify the ARPACK solutions with the commonly used iterative procedure and find excellent agreement of the order 10^{-16} .

IV. DISCUSSION OF RESULTS

We summarize our results for the mass spectrum and weak decay constants of the flavor-singlet and light-flavored vector mesons in Tables I and II, where the DSE and BSE are solved for two interaction, $\mathcal{G}(q^2)$, parameter sets in Eq. (5), namely $\omega = 0.4$ GeV and $\omega = 0.6$ GeV and the fixed value $\omega D = (0.8 \text{ GeV})^3$; see also discussion in Ref. [56]. In Table I, we list the 1^- masses for the ground state and first radial excitation following the Particle Data Group (PDG) conventions [69], whereas in Table II this is done for the weak decay constants.

A direct comparison of the mass and decay constant entries in both model-interaction columns reveals that the values obtained with $\omega = 0.4$ GeV are in much better agreement with experimental values of the 1^- ground states, namely in case of the ρ , $K^*(892)$, $\phi(1020)$ and J/ψ , whose ω dependence in the range $\omega \in [0.4, 0.6]$ GeV is rather weak. On the other hand, for $\omega = 0.6$ GeV the masses obtained for the radially excited states, $\phi(1680)$ and $\psi(2S)$, are only marginally better. It turns out that in the RL approximation, a realistic description of the radially excited vector meson masses is not possible with $\omega D = (0.8 \text{ GeV})^3$.

$J^P = 1^-$	$M_{V_n}^{\omega=0.4}$	$M_{V_n}^{\omega=0.6}$	$M_{V_n}^{\text{exp}} [69]$
$\rho^0(770)$	0.742	0.695	0.775
$\rho^0(1450)$	0.942	0.927	1.465
$K^*(892)$	0.951	0.914	0.896
$K^*(1410)$	1.217	1.206	1.414
$\phi(1020)$	1.087	1.055	1.019
$\phi(1680)$	1.295	1.376	1.659
J/ψ	3.114	3.065	3.097
$\psi(2S)$	3.393	3.507	3.689
$\Upsilon(1S)$	9.634	9.552	9.460
$\Upsilon(2S)$	9.945	9.848	10.023

TABLE I: Mass spectrum [in GeV] of flavor singlet and non-singlet mesons in the $J^P = 1^-$ channel. The model parameter ω refers to the interaction *ansatz* in Eq. (5), and we exemplify the spectrum for the values $\omega = 0.4$ GeV and $\omega = 0.6$ GeV with $\omega D = (0.8 \text{ GeV})^3$ fixed. We consider the ground state and first radial resonance, $n = 0, 1$, and compare with experimental values of the PDG [69] whose conventions we use in the last column.

We thus choose $\omega D = (1.1 \text{ GeV})^3$ and $\omega = 0.6$ GeV for which the numerical mass and decay constant values of the radially excited states are presented in Table III and compare well with experimental values, yet the ground states are no longer insensitive to ω variations for $\omega D = (1.1 \text{ GeV})^3$ [56]. In order to maintain $m_\pi = 0.138$ GeV, ω must increase beyond our reference value, $\omega = 0.6$ GeV, for the excited spectrum. These

$J^P = 1^-$	$f_{V_n}^{\omega=0.4}$	$f_{V_n}^{\omega=0.6}$	$f_{V_n}^{\text{exp.}}$
$\rho^0(770)$	0.231	0.242	0.221
$\rho^0(1450)$	—	—	
$K^*(892)$	0.287	0.304	0.217
$K^*(1410)$	0.195	0.127	
$\phi(1020)$	0.299	0.305	0.322
$\phi(1680)$	0.102	0.061	
J/ψ	0.433	0.463	0.416
$\psi(2S)$	0.208	0.230	0.295
$\Upsilon(1S)$	—	—	0.715
$\Upsilon(2S)$	—	—	0.497

TABLE II: Weak decay constants [in GeV] of flavor singlet and non-singlet $J^P = 1^-$ mesons; see Table I for explanations. Reference values for f_{V_n} are listed in the last column when available [69]. The long dash stands for numerically unstable results; i.e. the integral expression (14) does not stabilize with increasing numbers of Chebyshev moments. In the last column, experimental decay constants are extracted from the PDG values [69] using the formulae in Appendix A.

$J^P = 1^-$	M_{V_n}	f_{V_n}	$M_{V_n}^{\text{exp}}$	$f_{V_n}^{\text{exp.}}$
$\rho(1410)$	1.284	0.150	1.465	—
$\phi(1680)$	1.650	0.138	1.659	—
$\psi(2s)$	3.760	0.176	3.689	0.295
$\Upsilon(2s)$	10.140	0.564	10.023	0.497

TABLE III: Mass spectrum and weak decay constants for the first radially excited flavorless $J^P = 1^-$ states following PDG conventions. All values are in GeV and obtained with the interaction in Eq. (5) and the parameter values $\omega = 0.6$ GeV and $\omega D = (1.1 \text{ GeV})^3$. The long dash denotes numerically unstable results. In the first and fifth columns, experimental masses [69] and reference values for the decay constants f_{V_n} are given when available. Experimental values for f_{V_n} are extracted from the PDG [69] using the formulae in Appendix A.

results confirm an analogous trend observed for pseudoscalar mesons [53]. Nonetheless, the ground states are noticeably less dependent on the ωD values than the radial excitations where large mass differences are observed between both parameter sets. This agrees with the observations made in Refs. [53, 56] and extends them to the strange and charm vector mesons: the quantity $r_\omega := 1/\omega$ is a length scale that measures the range of the interaction's infrared component in Eq. (5). The radially excited states were shown to be more sensitive to long-range characteristics of $\mathcal{G}(q^2)$ than the ground states and we confirm that the mass of the radially excited states is lowered when r_ω decreases except in case of the $\phi(1680)$ and $\psi(2S)$ mesons.

The masses of the ground and the radial excitation states of the vector mesons we find correspond to the first and third eigenvalues (from highest to lowest), respectively. This is because the second eigenvalue does not correspond to 1^{--} states since the even Chebyshev moments are strongly suppressed. The exceptions are the $\rho(1450)$ using $D\omega = (1.1 \text{ GeV})^3$ and the $K^*(1410)$ with $D\omega = (0.8 \text{ GeV})^3$ and $\omega = 0.6$ where the radial excitation *does* correspond to the second eigenvalue. (NB: the radial excitations have identical quantum numbers as the ground state; therefore, the odd Chebyshev polynomials must be suppressed as it occurs for the ground states).

In summary, we do not find a parameter set that describes equally well the entire mass spectrum of ground and excited states, which demonstrates the insufficiency of this truncation and confirms our finding in the pseudoscalar channel [53].

V. CONCLUSION

We computed the BSAs for the ground and first excited states of the flavor-singlet and light-flavored vector mesons with an interaction *ansatz* that is massive and finite in the infrared and massless in the ultraviolet domain. This interaction is qualitatively in accordance with

the so-called *decoupling solutions* of the gluon's dressing function and thus supersedes the Maris-Tandy model [24] that vanishes at small momentum squared. In conjunction with the RL truncation, the latter proved to be a successful interaction model for the flavorless light pseudoscalar and vector mesons as well as quarkonia.

Motivated by the successful application of this interaction to the mass spectrum of light vector mesons as well as some of their excited states in Ref. [56], we extend this study to the strange and charm sectors and obtain the masses of ground and radially excited states as presented in Table I and also compute their weak decay constants. The numerical values obtained are in good agreement with experimental data in case of ground states, but the same parametrization yields values that compare poorly with experiment for the excited states. We thus confirm our earlier observation that no single parametrization of Eq (5) is suitable to reproduce the mass spectrum of both, the ground and excited states in RL truncation. Although not explicitly detailed here, this approximation also fails to produce the correct masses for the $D_{(s)}$ and $B_{(s)}$ vector mesons and the discrepancy is even more pronounced than in the case of charmed pseudoscalar mesons [53]. Reasons for this were put forward, e.g., in Ref. [61].

It has therefore become strikingly clear that a unified description of flavored pseudoscalar and vector mesons, quarkonia and their radial excitations can only be achieved within a treatment of the BSE beyond the leading truncation.

Acknowledgments

The work of F. Mojica and C. E. Vera was supported by *Comité Central de Investigaciones, Universidad del Tolima*, under project no. 60220516. E. Rojas acknowledges financial support from *Patrimonio Autónomo Fondo Nacional de Financiamiento para la Ciencia, la Tecnología y la Innovación, Francisco José de Caldas and Sostenibilidad-UDEA*. B. El-Bennich is supported by the São Paulo Research Foundation (FAPESP), grant no. 2016/03154-7, and by *Conselho Nacional de Desenvolvimento Científico e Tecnológico (CNPq)*, grant no. 458371/2014-9.

Appendix A: Extraction of the decay constants

Following Ref. [24, 70], we can extract the decay constant of the vector mesons from the experimental value [69] for the partial width of the $\rho, V \rightarrow e^+e^-$ decay, where V denotes the ϕ and heavy-flavored mesons.

$$f_\rho^2 = \frac{3m_\rho}{2\pi\alpha^2} \Gamma_{\rho \rightarrow e^+e^-},$$

$$f_V^2 = \frac{3m_V}{4\pi\alpha^2 Q^2} \Gamma_{V \rightarrow e^+e^-}. \quad (\text{A1})$$

In this expression, Q is the charge of the quarks in the meson and α is the fine structure constant.

-
- [1] I. G. Aznauryan *et al.*, *Int. J. Mod. Phys. E* **22**, 1330015 (2013).
- [2] I. C. Cloët and C. D. Roberts, *Prog. Part. Nucl. Phys.* **77**, 1 (2014).
- [3] V. P. Gonçalves, B. D. Moreira and F. S. Navarra, *Phys. Rev. D* **95**, no. 5, 054011 (2017).
- [4] B. El-Bennich, A. Furman, R. Kamiński, L. Leśniak and B. Loiseau, *Phys. Rev. D* **74**, 114009 (2006).
- [5] B. El-Bennich, A. Furman, R. Kamiński, L. Leśniak, B. Loiseau and B. Moussallam, *Phys. Rev. D* **79**, 094005 (2009) Erratum: [*Phys. Rev. D* **83**, 039903 (2011)].
- [6] O. Leitner, J.-P. Dedonder, B. Loiseau and B. El-Bennich, *Phys. Rev. D* **82**, 076006 (2010).
- [7] B. El-Bennich, J. P. B. C. de Melo, O. Leitner, B. Loiseau and J. P. Dedonder, *Prog. Part. Nucl. Phys.* **67**, 395 (2012).
- [8] B. El-Bennich, C. D. Roberts and M. A. Ivanov, *PoS QCD -TNT-II*, 018 (2012) [arXiv:1202.0454 [nucl-th]].
- [9] M. A. Paracha, B. El-Bennich, M. J. Aslam and I. Ahmed, *J. Phys. Conf. Ser.* **630**, no. 1, 012050 (2015).
- [10] V. M. Braun *et al.*, arXiv:1612.02955 [hep-lat].
- [11] B. El-Bennich, M. A. Ivanov and C. D. Roberts, *Nucl. Phys. Proc. Suppl.* **199**, 184 (2010).
- [12] B. El-Bennich, J. P. B. C. de Melo and T. Frederico, *Few Body Syst.* **54**, 1851 (2013).
- [13] E. O. da Silva, J. P. B. C. de Melo, B. El-Bennich and V. S. Filho, *Phys. Rev. C* **86**, 038202 (2012).
- [14] J. P. B. C. de Melo, K. Tsushima, B. El-Bennich, E. Rojas and T. Frederico, *Phys. Rev. C* **90**, no. 3, 035201 (2014).
- [15] G. H. S. Yabusaki, I. Ahmed, M. A. Paracha, J. P. B. C. de Melo and B. El-Bennich, *Phys. Rev. D* **92**, no. 3, 034017 (2015).
- [16] G. Krein, C. D. Roberts and A. G. Williams, *Int. J. Mod. Phys. A* **7**, 5607 (1992). doi:10.1142/S0217751X92002544
- [17] C. D. Roberts and A. G. Williams, *Prog. Part. Nucl. Phys.* **33**, 477 (1994).
- [18] R. Alkofer and L. von Smekal, *Phys. Rept.* **353**, 281 (2001).
- [19] C. S. Fischer and R. Alkofer, *Phys. Rev. D* **67**, 094020 (2003).
- [20] P. Maris and C. D. Roberts, *Int. J. Mod. Phys. E* **12**, 297 (2003).
- [21] C. D. Roberts and S. M. Schmidt, *Prog. Part. Nucl. Phys.* **45**, S1 (2000).
- [22] A. Bashir, L. Chang, I. C. Cloët, B. El-Bennich, Y. X. Liu, C. D. Roberts and P. C. Tandy, *Commun. Theor. Phys.* **58**, 79 (2012).
- [23] P. Maris and C. D. Roberts, *Phys. Rev. C* **56**, 3369 (1997).
- [24] P. Maris and P. C. Tandy, *Phys. Rev. C* **60**, 055214 (1999).
- [25] S. x. Qin, L. Chang, Y. x. Liu, C. D. Roberts and D. J. Wilson, *Phys. Rev. C* **84**, 042202 (2011).
- [26] S. X. Qin, L. Chang, Y. X. Liu, C. D. Roberts and S. M. Schmidt, *Phys. Lett. B* **722**, 384 (2013).
- [27] P. O. Bowman, U. M. Heller, D. B. Leinweber, M. B. Parappilly, A. G. Williams and J. b. Zhang, *Phys. Rev. D* **71**, 054507 (2005).
- [28] S. Furui and H. Nakajima, *Phys. Rev. D* **73**, 074503 (2006).
- [29] A. Cucchieri, T. Mendes, O. Oliveira and P. J. Silva, *Phys. Rev. D* **76**, 114507 (2007).
- [30] A. Cucchieri and T. Mendes, *PoS QCD -TNT09*, 026 (2009) [arXiv:1001.2584 [hep-lat]].
- [31] I. L. Bogolubsky, E. M. Ilgenfritz, M. Müller-Preussker and A. Sternbeck, *Phys. Lett. B* **676**, 69 (2009).
- [32] A. Sternbeck and M. Müller-Preussker, *Phys. Lett. B* **726**, 396 (2013).
- [33] O. Oliveira and P. J. Silva, *Phys. Rev. D* **86**, 114513 (2012).
- [34] O. Oliveira and P. Bicudo, *J. Phys. G* **38**, 045003 (2011).
- [35] P. Boucaud, J. P. Leroy, A. L. Yaouanc, J. Micheli, O. Pène and J. Rodríguez-Quintero, *Few Body Syst.* **53**, 387 (2012).
- [36] A. C. Aguilar and J. Papavassiliou, *JHEP* **0612**, 012 (2006).
- [37] A. C. Aguilar, D. Binosi and J. Papavassiliou, *Phys. Rev. D* **78**, 025010 (2008).
- [38] M. R. Pennington and D. J. Wilson, *Phys. Rev. D* **84**, 119901 (2011).
- [39] F. E. Serna, M. A. Brito and G. Krein, *AIP Conf. Proc.* **1701** (2016) 100018.
- [40] F. E. Serna, B. El-Bennich and G. Krein, arXiv:1703.09181 [hep-ph].
- [41] M. A. Bedolla, J. J. Cobos-Martínez and A. Bashir, *Phys. Rev. D* **92**, no. 5, 054031 (2015).
- [42] M. A. Bedolla, K. Raya, J. J. Cobos-Martínez and A. Bashir, *Phys. Rev. D* **93**, no. 9, 094025 (2016).
- [43] A. Krassnigg and P. Maris, *J. Phys. Conf. Ser.* **9**, 153 (2005).
- [44] M. Blank and A. Krassnigg, *Phys. Rev. D* **84**, 096014 (2011).
- [45] T. Hilger, M. Gómez-Rocha and A. Krassnigg, *Phys. Rev. D* **91**, no. 11, 114004 (2015).
- [46] T. Hilger, M. Gómez-Rocha and A. Krassnigg, arXiv:1508.07183 [hep-ph].
- [47] T. Hilger and A. Krassnigg, arXiv:1605.03464 [hep-ph].
- [48] T. Hilger, M. Gómez-Rocha, A. Krassnigg and W. Lucha, arXiv:1702.06262 [hep-ph].
- [49] M. Ding, F. Gao, L. Chang, Y. X. Liu and C. D. Roberts, *Phys. Lett. B* **753**, 330 (2016).
- [50] J. J. Dudek, R. G. Edwards, M. J. Peardon, D. G. Richards and C. E. Thomas, *Phys. Rev. D* **82**, 034508 (2010).
- [51] L. Liu *et al.* [Hadron Spectrum Collaboration], *JHEP* **1207**, 126 (2012).
- [52] G. K. C. Cheung *et al.* [Hadron Spectrum Collaboration], *JHEP* **1612**, 089 (2016).
- [53] E. Rojas, B. El-Bennich and J. P. B. C. de Melo, *Phys. Rev. D* **90**, 074025 (2014).
- [54] D. Binosi, L. Chang, J. Papavassiliou and C. D. Roberts, *Phys. Lett. B* **742**, 183 (2015).
- [55] D. Binosi, L. Chang, J. Papavassiliou, S. X. Qin and

- C. D. Roberts, Phys. Rev. D **95**, no. 3, 031501 (2017).
- [56] S. x. Qin, L. Chang, Y. x. Liu, C. D. Roberts and D. J. Wilson, Phys. Rev. C **85**, 035202 (2012).
- [57] E. Rojas, J. P. B. C. de Melo, B. El-Bennich, O. Oliveira and T. Frederico, JHEP **1310**, 193 (2013).
- [58] B. El-Bennich, E. Rojas, M. A. Paracha and J. P. B. C. de Melo, AIP Conf. Proc. **1625**, 80 (2014).
- [59] E. Rojas, B. El-Bennich, J. P. B. C. De Melo and M. A. Paracha, Few Body Syst. **56**, no. 6-9, 639 (2015).
- [60] P. Maris, C. D. Roberts and P. C. Tandy, Phys. Lett. B **420**, 267 (1998).
- [61] B. El-Bennich, G. Krein, E. Rojas and F. E. Serna, Few Body Syst. **57**, no. 10, 955 (2016).
- [62] M. Bhagwat, M. A. Pichowsky and P. C. Tandy, Phys. Rev. D **67**, 054019 (2003),
- [63] A. Höll, A. Krassnigg and C. D. Roberts, Phys. Rev. C **70**, 042203 (2004).
- [64] B. El-Bennich and E. Rojas, EPJ Web Conf. **113**, 05003 (2016).
- [65] J. Segovia, B. El-Bennich, E. Rojas, I. C. Cloët, C. D. Roberts, S. S. Xu and H. S. Zong, Phys. Rev. Lett. **115**, no. 17, 171801 (2015).
- [66] S. S. Afonin and I. V. Pusenkov, Phys. Rev. D **90**, no. 9, 094020 (2014).
- [67] R. B. Lehoucq, D. C. Sorensen, C. Yang, *ARPACK Users' Guide: Solution of Large-Scale Eigenvalue Problems with Implicitly Restarted Arnoldi Methods* (Society for Industrial & Applied Mathematics, 1998).
- [68] W. H. Press, S. A. Teukolsky, W. T. Vetterling and B. P. Flannery, ISBN-9780521430647.
- [69] C. Patrignani *et al.* [Particle Data Group], Chin. Phys. C **40**, no. 10, 100001 (2016).
- [70] H. M. Choi, C. R. Ji, Z. Li and H. Y. Ryu, Phys. Rev. C **92**, no. 5, 055203 (2015).